J Mater Sci (2009) 44:154–159
DOI 10.1007/s10853-008-3119-7

Synthesis of submicron sized silver powder for metal deposition via laser sintered inkjet printing

K. C. Yung · S. P. Wu · H. Liem

Received: 1 September 2008 / Accepted: 12 November 2008 / Published online: 27 November 2008

Abstract Submicron sized silver powder was prepared from $AgNO_3$ using a chemical-reduction method. A spherical silver power exhibiting an average particle size distribution of 0.2–0.4 μm and an excellent dispersibility was achieved and applied to the inkjet printing process. A drop-on-demand (DOD) inkjetting system was used to print the silver particles suspended in a terpineol solvent. Through sintering at 300 °C, the size of the particles adjacent to the borderline of droplets were gradually increased and necking was observed between the droplets. Alternatively, the substrate for the particles could be heated to a lower temperature, and the sintering process of the conducting line was completed by the application of a laser beam. Increase in the laser power reduces the resistivity of the line. Through microstructure analysis, the necks between droplets were sintered at a specific energy density ($\psi = 0.0398$ J mm^{-3}). The conducting lines were soldered and of a larger aggregation, between which a discontinuous micro-crack was observed. This was attributed to the surface tension effect and shrinkage during solidification. Influence of the densification parameters on resistivity was significant.

Introduction

The development of direct printing of functional materials has aroused significant attention as an alternative to the conventional integrated circuit (IC) process, especially in the area of low cost flexible electronics. Since the drop-on-demand (DOD) inkjet printing is an additive process, many problems can be alleviated in a cost-effective manner. The full data driven and mask-less nature of DOD inkjet processing allows more versatility than other direct printing methods. The material is deposited in a carrier solution on the substrate by a piezo electrically driven micro capillary tube. This solution processing provides enhanced flexibility for choosing both the depositing material and the substrate.

In the case of making electrically conductive lines, nano-sized noble metal like gold was used [1, 2]. Nanoparticles were used to illustrate the significant depression of sintering temperature due to the thermodynamic finite size effect and the relatively low desorption temperature of the surface monolayer. Dockendorf et al. [3] and Ko et al. [4] demonstrated that inter-connectors and multilayers could be fabricated using laser sintering of gold nanoparticle. Sawyer [5] reported that a planar, cantilevered heatuator was printed on a glass slide using a silver nanoparticle as the conductive material.

From the practical point of view, submicron silver particle is a promising functional material for inkjet printing application due to its reasonable price, high electrical conductivity, strong resistance to oxidation and simple synthesis process [6]. In the inkjet printing process, it is a prerequisite to use submicron sized non-agglomerated silver particles to hinder the deposition of particles from ink, and prevent the nozzle from clogging.

In this Letter, we report a chemical reaction method for the formation of submicron silver powder particles that are employed as a conductive filler of ink for inkjet printing. The ink deposition was carried out by DOD printing using a commercial piezo inkjet head (Microdrop MD-K-140-H). The inkjet printed samples were cured using a frequency tripled Nd-YAG laser. Subsequently, the bulk resistivity and microstructures of the sintered conductive lines were investigated.

K. C. Yung (✉) · S. P. Wu · H. Liem
Department of Industrial and Systems Engineering, The Hong Kong Polytechnic University, Hung Hom, Kowloon, Hong Kong
e-mail: mfkcyung@inet.polyu.edu.hk

Experimental set-up

Preparation of submicron sized silver particles

Chemicals having reagent grade quality were used without further purification. Silver powders were obtained by a reaction of $[Ag(NH_3)_2]^+$ complex with hydrazine hydrate. In a typical preparation of silver powders, $AgNO_3$ ($\sim$11.2 g) and aqua ammonia (50 mL) were mixed and then diluted to 400 mL. This solution was added drop-wise for 60 min to a stirred solution (400 mL) containing 12 g of hydrazine hydrate and dispersion agent. The temperature was kept at 60 °C. The metallic powders were separated from the solution, washed and dried, subsequently.

Inkjet printable silver conductor

The essential functional material in the ink was as-prepared silver powders. All of the inkjet printed devices reported here were fabricated using a desktop piezo-driven inkjet print head (Microdrop MD-K-140-H) with an orifice diameter of 70 μm manufactured by Microdrop Technologies GmbH. As the head was fixed, structures were printed through a computerized substrate movement at a rate of 10 mm/s and at a distance of 5 mm below the head. Table 1 summarises the parameters for the print head to continuously inject droplets onto the substrate.

The substrate was heated from 100 to 150 °C by a hotplate during the deposition process to improve deposit quality. By heating the substrate, the liquid in the droplets was flash-evaporated on contact. The rapid liquid evaporation also eliminated wetting problems.

Laser sintering of silver conductor

A frequency tripled Nd-YAG laser, lowering its original wavelength to 355 nm, was irradiated at the centre of a printed line to define a finer feature. The beam was defocused by 10 mm to avoid over-heating (carbonization) of the PI substrate. The substrate was placed on a translation stage and in situ images were taken via a fixed (200×) microscope. The laser power and wavelength have to be appropriately selected to melt the nanoparticles to produce silver conductors. As discussed in a number of previous work [7, 8], laser power is an important factor affecting cross sectional area as well as the bump height of the circuit line. Over-dosage of laser power will have high thermal damage resulting in a very rough surface. Laser power should also be selected to avoid deformation of substrates. Laser wavelength is also important as the reflectivity of a metal with an incident laser beam is dependent on laser wavelength. This reflectivity is an important factor for the heat input in the laser sintering (curing) process. In a previous study [7], a reduced reflectivity of 50% can lead to an overall temperature increase and the maximum temperature in the centre can be increased from 1,400 to 1,700 °C.

Table 1 Stable jetting parameter

Voltage/V	Pulse width/μs	Repetition time/μs	Display period/s	Head temperature/°C
100	40	404	90	70

Characterisation

Direct observations of the powders and microstructure of the conductor were analysed by scanning electron microscopy (SEM) on a Lecia Steroscan 440. The crystal structure was characterised by an X-ray diffraction XL30δDX-4i (Philips). Thermogravimetry (TG) and differential scanning calorimetry (DSC) were carried out at scanning rates of 5 °C/min in a flowing air environment.

Results and discussion

Chemical reaction and material characterisation

To obtain submicron sized silver powder particles, $[Ag(NH_3)_2]^+$ complex was reduced by hydrazine hydrate. In this process, the following chemical reaction occurred:

$$2[Ag(NH_3)_2]^+ + N_2H_4 \rightarrow 2Ag + N_2 + H_2 + 2NH_4^+ + 2NH_3 \quad (1)$$

In the course of the reaction, addition of dispersed $[Ag(NH_3)_2]^+$ droplet into the dispersed ascorbic acid is important because a confined amount of silver ion in a droplet of $[Ag(NH_3)_2]^+$ may govern the size of silver powders. A dispersion agent can prevent powder particles from coming together due to electrostatic force, surface tension and space hindrance effects.

Figure 1 shows the XRD pattern of the powder prepared by the solution containing $AgNO_3$ and ascorbic acid. It can be noted that the diffractogram exhibits the characteristic peaks of crystalline metallic silver (cubic) with d (Å) = 2.359, 2.043, 1.444 and 1.231, respectively, which were very close to that given by the JCPDS file no. 4-0783 with d (Å) = 2.359, 2.044, 1.445 and 1.231.

In practical application of inkjet printing, powder particles with an average size of 0.3–0.5 μm and good dispersibility are important to avoid clogging of the nozzle. It was reported that finer powder provided a larger surface area to absorb more laser energy, which increased the

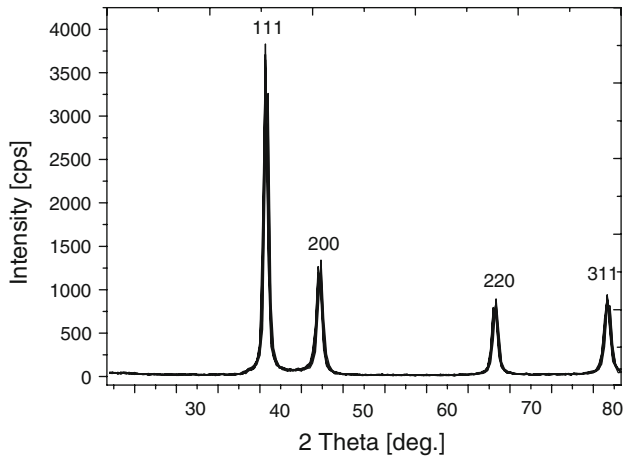

Fig. 1 XRD spectrum of submicron silver powders

working temperature and thus the sintering kinetics. It was further reported that laser sintering of finer particles tends to enhance the kinetic of densification, which is very important to improve the conductivity.

However, if the average particle size was less than 100 nm, the metal layer contracted excessively when the conductor was laser sintered, so that it became porous and/or cracked, resulting in significant high resistivity. Considering the high stability of the ink and the low resistivity of the conductor, we chose as-prepared monodispersed submicron sized silver powder of 3.4 $m^2 g^{-1}$. Figure 2 presents the SEM photo of this powder, which has an aggregate size of 207 nm and specific area of 3.4 $m^2 g^{-1}$.

Metallic silver particles were analysed by TG/DSC in an air flow. Figure 3 shows the TG/DSC thermograms obtained at a heating rate of 10 °C/min. According to the TG analysis, the oxidation of silver was not significant; however, a sharp exothermal peak appeared at 300 °C, indicating a fast weight loss of the sample. This was due to

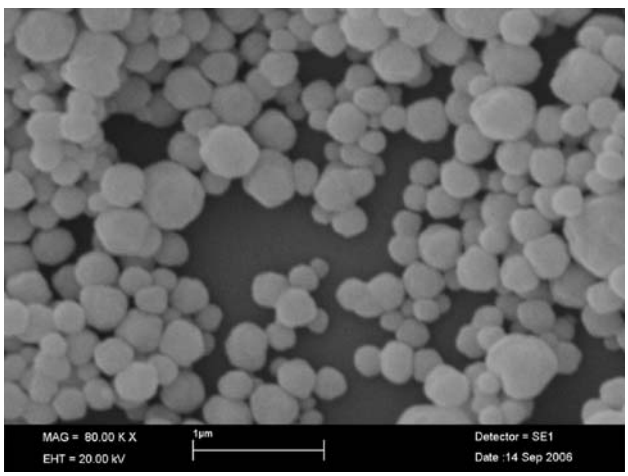

Fig. 2 SEM morphology of submicron silver powders

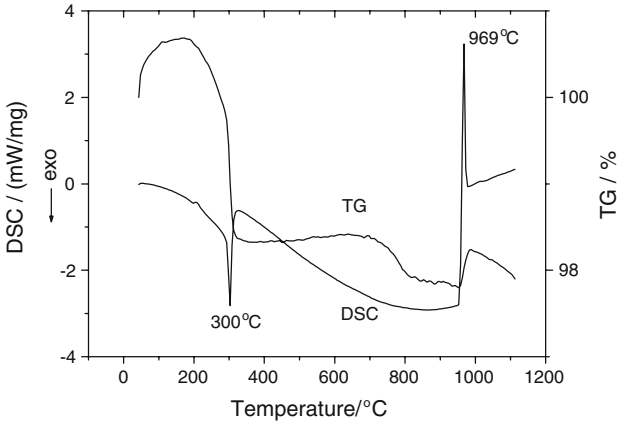

Fig. 3 DSC thermograms of ultra fine silver powders

the decomposition of silver oxide. The featured endothermal peak at 956.9 °C indicated the melting of silver.

Preparation of ink for inkjet printing

The ink used in inkjet printing consisted of primarily two functional constituents: (1) conductive phase, the as-prepared silver powder having an excellent dispersibility, and (2) organic phase, which disperses the metal and binder component to reserve the desired rheological properties for the ink.

The stability of the ink is one of the important parameters that ensures the quality of thick films, because the ink is normally stored for a long time prior to use. The rheological behaviour is primarily controlled by the nature of powder, dispersion process and solvent. The organic solvent plays an important role in wetting the powder surface. The solvent provides a homogeneous suspension of the particles of the functional materials, leading to a good rheology suitable for the inkjet process. Higher viscosity solvents having low evaporation rates are preferred. Solvents with high evaporation rates such as isopropyl alcohol can be used in printing for only a few minutes before the nozzle is clogged with dried ink. Thus, Terpineol is selected as a solvent in this work due to its higher boiling point $\sim$220 °C and larger viscosity $\sim$54 mPa S.

The ink was prepared by dispersing 10% by weight of silver particle in Terpineol. Higher concentration led to lower ink stability and caused excessive clogging. The same nozzle from a given head was used for the whole experiment. The print head was heated to 70 °C using a power resistor to lower the ink viscosity within a specific range such that the ink was compatible with the print head. The feed system contained enough ink in the cavity so as to ensure continuous operation longer than 1 hour. The diameter of each injected droplet could range from 100 to 250 μm, depending on the strength of the driving pulse.

In our experiments, the substrate was heated to 300 °C using a heated plate, the inkjet droplets having submicron sized particles were expelled at the minimum driving voltage. The produced droplets had a diameter of ~120–150 μm and a borderline height of ~0.8–1 μm, which was about 3–5 particles height (see Fig. 4). From Fig. 4a, it is observed that the particles are intensively distributed along the circumference of a droplet due to surface tension effect. The microstructure of this ring is further examined in Fig. 4b. A particle size distribution is incorporated, and necking rather than complete melting between droplets is observed. By virtue of surface tension, some dumbbell-shaped particle agglomeration can be found. This is very similar to the morphology of an initial stage in the typical sintering process. Although the melting point (T_m) of bulk silver is high as revealed by TG/DSC analysis, the required sintering temperature (T_s) is as low as 300 °C due to small particle size effect.

Sintering of nano-sized silver particles is observed to occur in the range of 130–140 °C due to the thermo-dynamic finite size effect [9]. The sintering initiating temperature (T_s) is used to compared with the melting temperature (T_m) of bulk silver (969 °C).

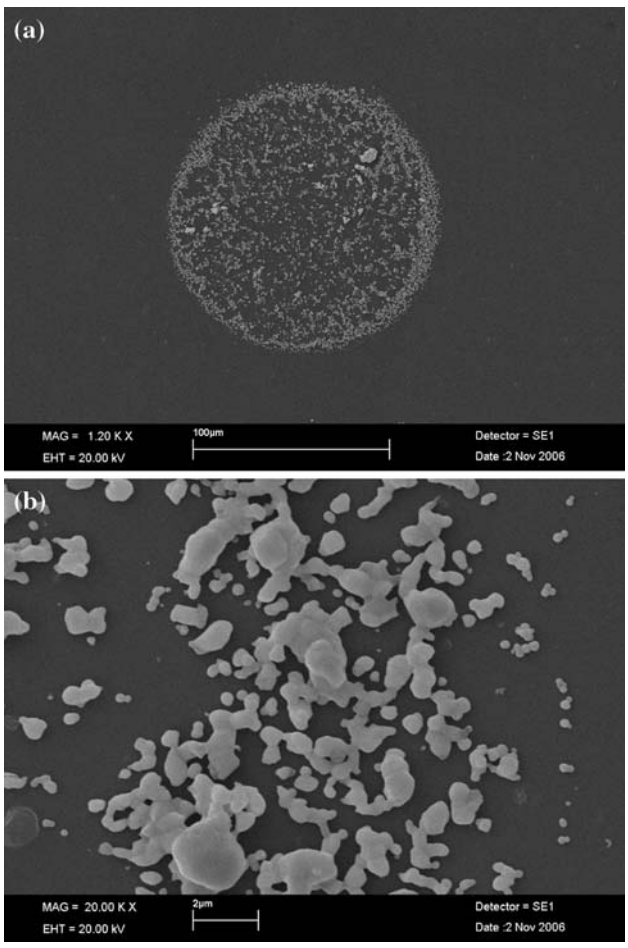

Fig. 4 An inkjet printed droplet of submicron sized particle silver on a PI substrate after being sintered, imaged by SEM. **a** An overhead view. **b** A microstructure of borderline

Bulk resistivity of laser sintered conductor

For multi-layer deposition, print-on-the fly mode was used (i.e., constant relative movement), where the pitch is determined by the ejection frequency and substrate velocity. Multiple layers are thus printed line-wise on top of each other. After the deposition of the silver submicron sized particle ink on a heated substrate by the DOD inkjet printing, Nd:YAG laser pulses (0.1–1.0 W) were employed to sinter the lines.

The substrate was heated to a lower temperature, such as 120 °C, so that multiple droplets flowed together before the solvent evaporated and a conducting line was sintered with a very uniform cross section. The laser spot size was 80–230 μm depending on the different laser powers applied. The dependence of bulk resistivity on the laser power is presented in Fig. 5. It is generally accepted that the conductivity of conductive film depends upon metallic particle behaviour and the contact area between conductive filling materials. The resistivity (ρ) is calculated from the relation RA/L, where the resistance R was measured by a micro-needle probe station, A was the cross sectional area of the silver line measured by SEM and L was the length of the test sample (3 cm). Laser power was varied from 0.2 to 0.8 W to study the resistivity change (Fig. 5). Significant brightness change was observed when the laser power was above 0.2 W. Polyimide film deformed significantly for power exceeding 1 W, which was able to vaporize silver particles effectively. At lower power, the sintering process was not complete and the resistivity was still high. The resistivity decreased dramatically around 0.4 W and did not show much deviation above 0.6 W. The minimum

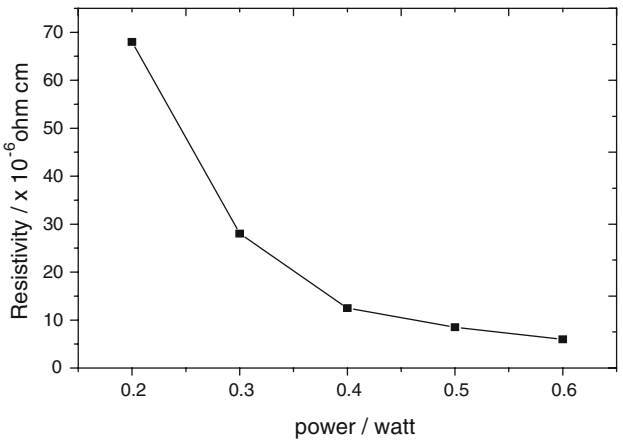

Fig. 5 Influence of laser power on bulk resistivity of silver conductor

measured resistivity (8 μΩ m) obtained from sintering was almost five times higher than that of the bulk (1.6 μΩ cm). The finite conductivity is suggestive of the trapping of organic solvent in the metal and/or incomplete sintering of the metal particles.

According to the so-called *percolation threshold* effect, the bulk resistivity of silver conductor depends also on the contact area between conductive particles; that is to say, more contact areas result in a less bulk resistivity. Norton reported that the increased film density reduced the electrical resistivity as the degree of contact between particles was increased [9]. Simchi reported that the sintered density depended on both powder characteristics and the fabrication parameters. In general, as the energy input increases (higher laser power or lower scan rate) higher density is obtained [10], producing a low bulk resistivity.

Microstructure of silver conductor

According to the literature [11], the most critical parameters determining the intensity and energy delivered to a single layer of powder having a thickness (h) are the laser power (P), laser beam spot size (d), scan rate (v), scan line spacing (w) and geometrical scanning strategy including the length of scan vector and the method of irradiation between each successive layer.

This energy rapidly heats up the particles above their melting point and causes particle bonding to occur. Therefore, the apparent sintering temperature (T_s) in a very simple form is related to the relevant process parameters as:

$$T_s = T_o + \frac{1}{C}\left[\left(\frac{\pi\eta}{4\rho}\right)\left(\frac{p}{hvw}\right) - \Delta H\right] \quad (2)$$

The specific energy input (ψ) as the total energy input per volume of each sintered track was defined according to Eq. 2.

$$\psi = \frac{p}{hvw} \quad (3)$$

Therefore, it can be deduced that ψ is in direct relation to T_s. With an increase in the laser power (P), the sintering temperature (T_s) increased.

The amount of densification (D) can be related to the specific energy input as given in Eq. 3:

$$\ln(1 - D) = -k\psi \quad (4)$$

where k is designated as the densification coefficient which is related to chemical constitutions, particle size and particle distribution. It is noteworthy that this relation is valid only when particle bonding is formed by full melting/solidification. When materials and other laser sintering parameters were fixed, it can be calculated that D increases with increasing ψ.

The connectivity and orientation of the particles depend upon the processing condition. The microstructure of the laser sintered sample illuminated by different laser powers ranged from 0 to 0.7 W are illustrated in Fig. 6. Figure 6a shows the inkjetting printed line before sintering. It is observed that there is organic solvent filled in the gap between particles, and thus the line surface is relatively smooth. After the sample was sintered at 0.3 W laser power, we obtained $h = 0.5$ mm, $v = 160$ mm s^{-1} and $w = 0.13$ mm by optical micrograph analysis. The specific energy input ψ was calculated to be 0.0288 J mm^{-3}. Since Terpineol was vaporised despite its high boiling point, a wavy surface and some microcracks appeared due to surface shrinkage. Limited inter-connectivity between particles was observed. The densification of the sintered line was low and several pores appeared. The pores were elongated horizontally as seen in Fig. 6b. When the laser power was increased up to 0.5 W ($h = 0.5$ mm, $v = 160$ mm s^{-1}, and $w = 0.194$ mm), the specific energy input ψ was calculated to be 0.0322 J mm^{-3}. The growth of particles was visually significant due to good inter-connectivity between silver particles by laser sintering, forming a continuous network of inter-connected silver particles. Figure 6c shows the necks between the particles sintered at 0.7 W ($h = 0.5$ mm, $v = 160$ mm s^{-1} and $w = 0.224$). The specific energy input ψ was calculated to be 0.0398 J mm^{-3}. Thus, the necks were formed with this energy, and the particles were practically soldered, forming a large aggregate, between which a discontinuous micro-crack appeared, which was attributed to the surface tension effect and solidification shrinkage. High thermal gradients induced large thermal stresses inside the materials, and thus may cause delamination of the sintered layer. The densification was high, and it significantly increases the conductivity of the silver conductor.

Figure 6d shows the SEM image performed on the cross section of a conductor. It is observed that a line with a very uniform cross section is achieved. Using this SEM image, the thickness is estimated to be about 1 μm. Compared with the morphology of particles on the top surface (see Fig. 6c), a single particle cannot be observed on the conductor, which was very similar to that of the top of the cross section. However, several spherical silver particles were observed at the interface between the conductor and the substrate. The possible explanation is that the typical scan rate used in laser sintering process is about 160 mm s^{-1}; thus, the heat flow distance during the interaction time is less than the particle diameter, leading to very fast heating up of the particle surface. The absorbed energy is then dissipated to the surrounding area by thermal diffusion. As a result, after penetrating 1 μm into the silver layer, the energy was not enough to sinter the particles underneath.

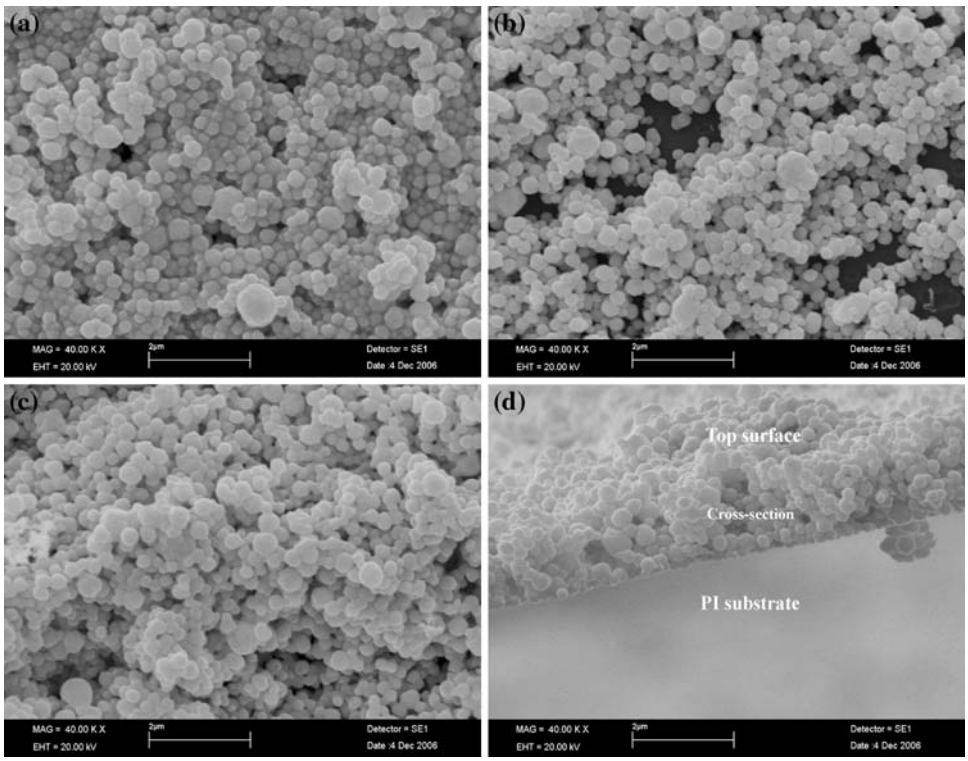

Fig. 6 Microstructure of silver conductor sintered by laser at different power. Power/Watt **a** 0, **b** 0.3, **c** 0.7, **d** 0.7—Cross section

In general, the degree of densification is important in determining the electrical resistivity of thick film. This study revealed the fact that higher inter-connectivity between particles can be achieved by increasing the laser sintering power. This results in a higher densification of the material and thus a lower resistivity. This phenomenon is suggested by SEM analysis.

Conclusions

Submicron sized silver powder particles were synthesized using a chemical-reduction method. Powders with an average particle size of 0.2–0.4 μm and excellent dispersibility were achieved. A DOD inkjetting system was used to print the as-prepared silver powder particles suspended in a Terpineol solvent. The diameter and borderline height of a typical droplet were measured to be 120–150 μm and 0.8–1 μm, respectively. The particles in borderline were sintered at 300 °C. Alternatively, the substrate could be heated to a lower temperature and the lines were sintered by using a laser. As the laser power increased, the resistivity of the conductive line decreased. By microstructure analysis, the presence of necks between particles sintered at high laser power was considered to be a common phenomenon. Upon being soldered, the silver particles formed a large aggregation, between which a discontinuous microcrack was observed. This was attributed to the surface tension effect and solidification shrinkage. Last, the densification was explicitly related to the specific energy input (ψ) during laser sintering.

References

1. Bieri NR, Chung J, Haferl SE, Poulikakos D, Grigoropoulos CP (2003) Appl Phys Lett 82(20):3529
2. Chung J, Ko S, Bieri NR, Grigoropoulos CP, Poulikakos D (2004) Appl Phys Lett 84(5):801
3. Dockendorf C, Choi T, Grigoropoulos CP, Poulikakos D (2005) Multilayer direct writing of electrical conductors with gold nanoinks using the fountain-pen principle. In: Proceedings of the ASME IPACK, San Francisco, CA, USA, 17–22 July 2005
4. Ko S, Chung J, Pan H, Grigoropoulos CP, Poulikakos D (2006) Fabrication of multilayer passive electric components using inkjet printing and low temperature laser processing on polymer. In: SPIE Photonics West, San Jose, CA, USA, 21–26 Jan 2006
5. Feller SB, Wilhelm EJ, Jacobson JM (2002) J Microelectromech Syst 11(1):54
6. Wu SP, Meng SY (2005) Mater Chem Phys 89:423
7. Bieri NR, Chung J, Poulikakos D, Grigoropoulos CP (2005) Appl Phys A-Mater Sci Process 80:1485
8. Cédric D, Poulikakos D, Hwang G, Nelson B, Grigoropoulos CP (2007) Appl Phys Lett 91:243118
9. Moon KS, Dong H, Maric R et al (2005) J Electron Mater 34(2):168
10. Norton MG (1991) J Mater Sci 26:2322. doi:10.1007/BF01130176
11. Simchi A (2006) Mater Sci Eng A 428:148